A Platinum Open Access Journal for Organic Chemistry

Paper

Free to Authors and Readers | DOAJ Seal | *Arkivoc* **2022**, part iii, 66-84

Unusual ionization of phosphine-boranes under RP-HPLC-HRMS conditions disclose a potential system for reduction of C=O bond

Sylwia Sowa,[a] Ewelina Buczak,[b] Paweł Woźnicki,[a] Olga Bąk,[c] Piotr Borowski,*[d] Beata Herbaczyńska-Stankevič,[a] and Marek Stankevič*[a]

[a]Department of Organic Chemistry, Institute of Chemical Sciences, Faculty of Chemistry, Maria Curie-Skłodowska University in Lublin, 33 Gliniana st., 20-614 Lublin, Poland
[b]Minisynthesis Team, Łukasiewicz Research Network – Industrial Chemistry Institute, 8 Rydygiera st., 01-793 Warsaw, Poland
[c]Department of Chromatographic Methods, Institute of Chemical Sciences, Faculty of Chemistry, Maria Curie-Skłodowska University in Lublin, 3 Marie Curie-Skłodowska sq., 20-031 Lublin, Poland
[d]Department of Theoretical Chemistry, Institute of Chemical Sciences, Faculty of Chemistry, Maria Curie-Skłodowska University in Lublin, 3 Marie Curie-Skłodowska sq., 20-031 Lublin, Poland
Email: marek.stankevic@mail.umcs.pl piotr.borowski@mail.umcs.pl

This paper is dedicated to Professor Gyorgy Keglevich on the occasion of his 65th birthday

Received 03-18-2022 **Accepted Manuscript** 05-14-2022 **Published on line** 05-22-2022

Abstract

HRMS analysis of a set of phosphine-boranes using RP-HPLC-HRMS has been performed using an acetonitrile/water mixture. The data show that all compounds undergo ionization under the measurement conditions to afford cations of $[M-H]^+$, $[2M-H]^+$, $[2M-3H]^+$, $[2M-5H]^+$ or $[2M\ 6H]^{2+}$ type. A detailed analysis of their structures led to the conclusion that these species might act as carbonyl-group activators.

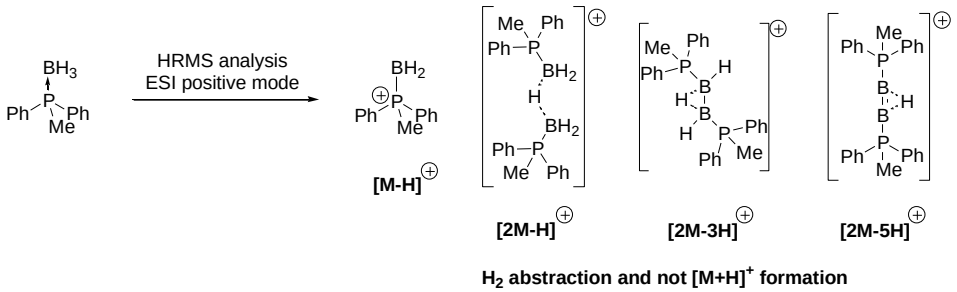

Keywords: Phosphine-boranes, HPLC-HRMS, ionization, DFT analysis

Introduction

Phosphine-boranes have emerged as a new and valuable class of organophosphorus compounds in the past few decades.[1,2] Due to the presence of a weak P–B bond, these compounds are regarded as good substitutes for free phosphines because they lack the disadvantages of the latter. Their utility as substrates has been proven many times, especially in the synthesis of P–stereogenic diphosphine ligands for asymmetric catalysis.[3-6] The presence of a weak phosphorus-boron bond frequently raises the problem of the complete analysis of phosphine–boranes, however, especially when the data are collected for the preparation of a manuscript. Contrary to NMR, which is regarded as a non-destructive analytical method, MS analysis, especially the coupled LC–MS or GC–MS techniques, causes cleavage of the P–B bond predominantly, leading to the corresponding free phosphines during measurements. The latter may undergo oxidation, affording a completely different compound which enters the mass analysis. As a consequence, a detailed description of mass peaks should be included in the analysis.

An analogous problem is associated with the identity confirmation, which is usually associated with either elemental analysis or high-resolution mass spectrometry (HRMS). Many phosphine–boranes exist as oils which strongly influence results reliability using elemental analysis. Therefore, HRMS should be the method of choice for identity confirmation for these compounds.

Herein, we present the results concerning the HRMS analysis of a set of structurally-different phosphine–boranes using a RP–HPLC–HRMS technique, along with some interesting consequences associated with the discussed observations.

Results and Discussion

All compounds used for RP–HPLC–HRMS analysis are presented in Figure 1. Some of them have been prepared as presented in Scheme 1.

In Scheme 1, the phosphine–boranes **20** and **21**, possessing a hydroxy substituent at the γ carbon atom, were prepared from **2** using a deprotonation/epoxide-addition sequence. Phosphine–boranes **27** and **28** were obtained from 1-indanone, which was subjected to a reaction with a base followed by an addition of Ph_2PCl and BH_3 complex. The obtained compound **27** was treated with $NaBH_4$ in methanol, affording the final phosphine–borane **28**. Phosphine–borane **29**, with an ester functionality, has been obtained from the corresponding secondary phosphine–borane **32** by treatment with ethyl chloroacetate in the presence of a base. Finally, triarylphosphine–borane **30** has been prepared by simple reaction of a free phosphine **33** with BH_3 complex.

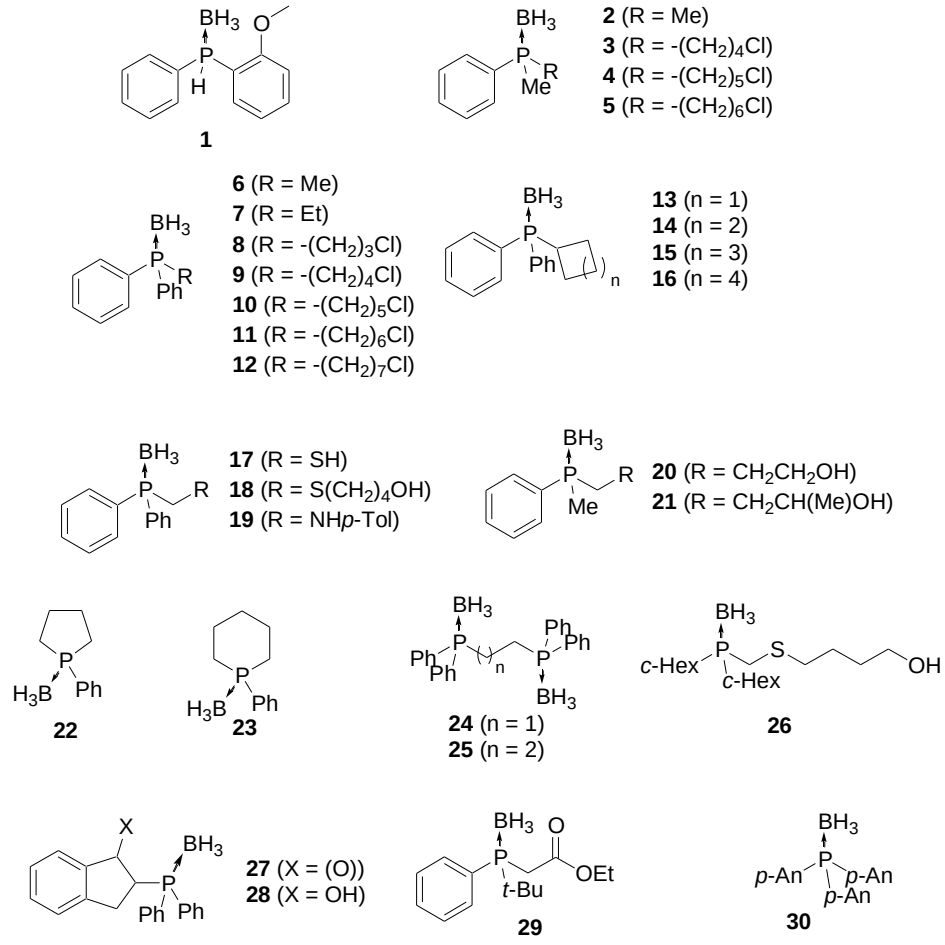

Figure 1. A set of phosphine–boranes used for HRMS analysis.

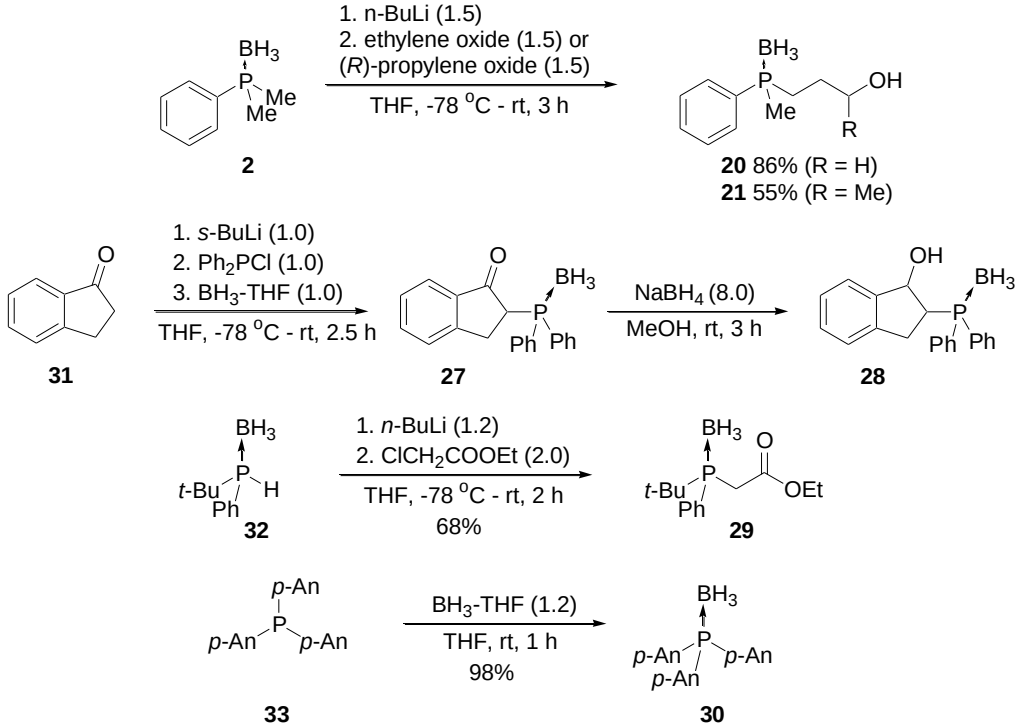

Scheme 1. Synthesis of **20**, **21**, **27**, **28**, **29** and **30**.

All phosphine–boranes were subjected to HRMS analysis using a RP–HPLC–HRMS technique. Samples were dissolved in MeOH and subjected to HPLC analysis with 5% or 30% MeCN in water as eluent in an isocratic mode, followed by HRMS analysis with ESI mode and IT–TOF mass-peak analysis. For better ionization of the analyzed compounds, formic acid was added to each solvent (1mL/L). The analysis of each compound shows an interesting feature which is depicted in detail for diphenylmethylphosphine–borane **6** in Figure 2.

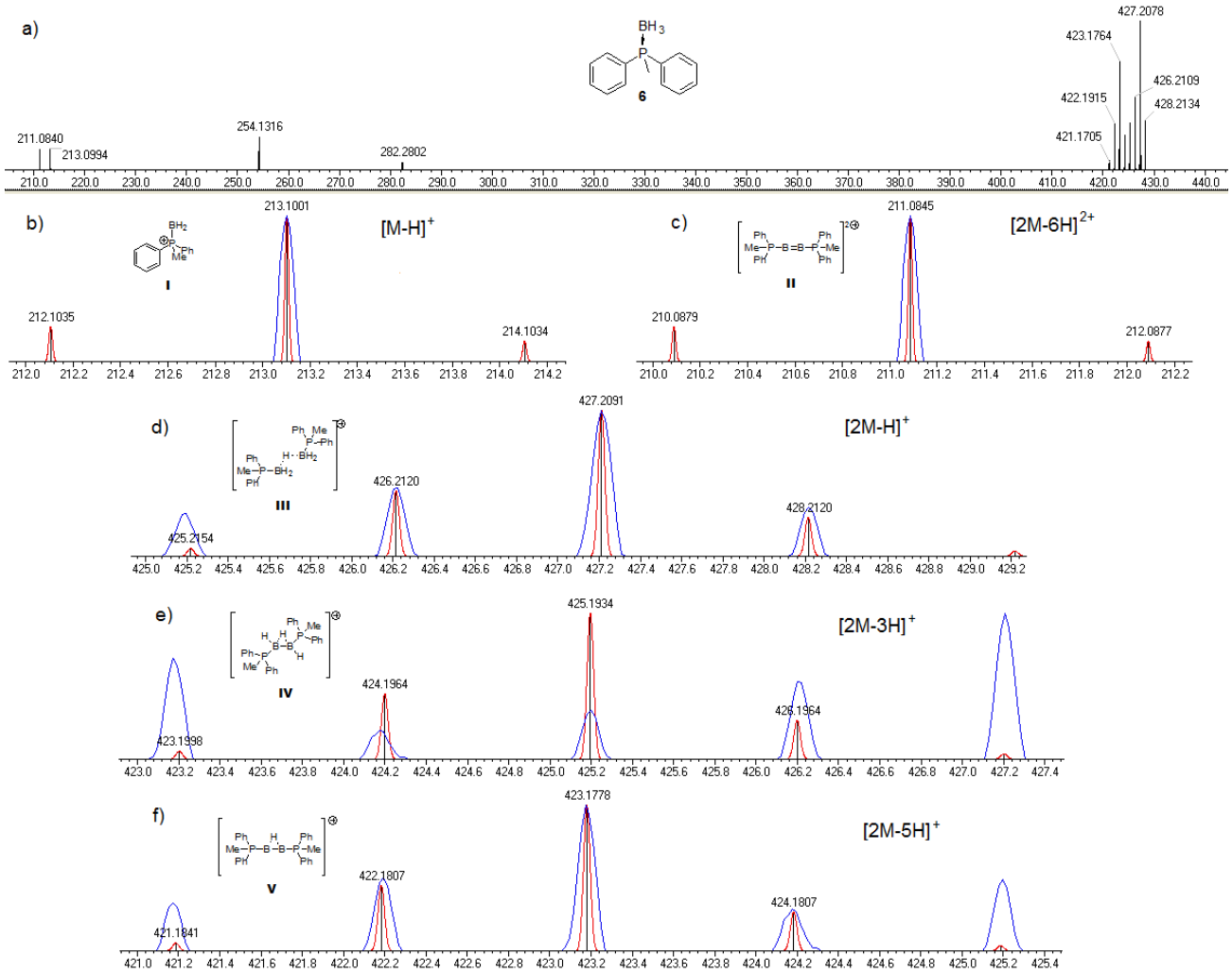

Figure 2. RP-HPLC-HRMS analysis of **6**. Theoretical mass peaks are depicted in red. a) The overall mass spectrum. b) Mass peak for $[M–H]^+$. c) Mass peak for $[2M–6H]^{2+}$. d) Mass peak for $[2M–H]^+$. e) Mass peak for $[2M–3H]^+$. f) Mass peak for $[2M–5H]^+$.

The results presented in Figure 2 show that none of the mass peaks found for phosphine–borane **6** are of M+H–type. The mass peak closest to the molecular mass of **6** was *m/z* 213.1001 which corresponds to the molecular peak of $Ph_2MeP(BH_2)$ cation **I** (Figure 2b). This peak, however, was weak compared to the other peaks found in the spectrum. The most intensive peak was found at *m/z* 427.2091, which corresponds to **III**, an adduct of the starting phosphine–borane **6** and $Ph_2MeP(BH_2)$ cation (Figure 2d). There are two more mass peaks found in this region. The first was found at *m/z* 425.1934, and corresponds to the compound **IV** derived through the formal elimination of a hydrogen molecule from **III** (Figure 2e). The second mass peak was found at *m/z* 423.1778, which corresponds to the compound **V**, derived through the formal elimination of a hydrogen molecule from **IV** (Figure 2f). Finally, there was still one weak mass peak found at *m/z* 211.0845

which was ascribed to a dication **II**. This dication is formally formed by hydrogen-molecule elimination from cation **I**, followed by dimerization of the formed intermediates (Figure 2b). The analysis of the spectra shown in Figure 2a revealed that the most intense mass peaks corresponded to a few dimers of different composition. Moreover, it seemed that hydrogen abstraction is a quite facile process, at least under the measurement conditions.

In order to understand the mechanism of the transformation of **6**, DFT calculations have been performed (Scheme 2).

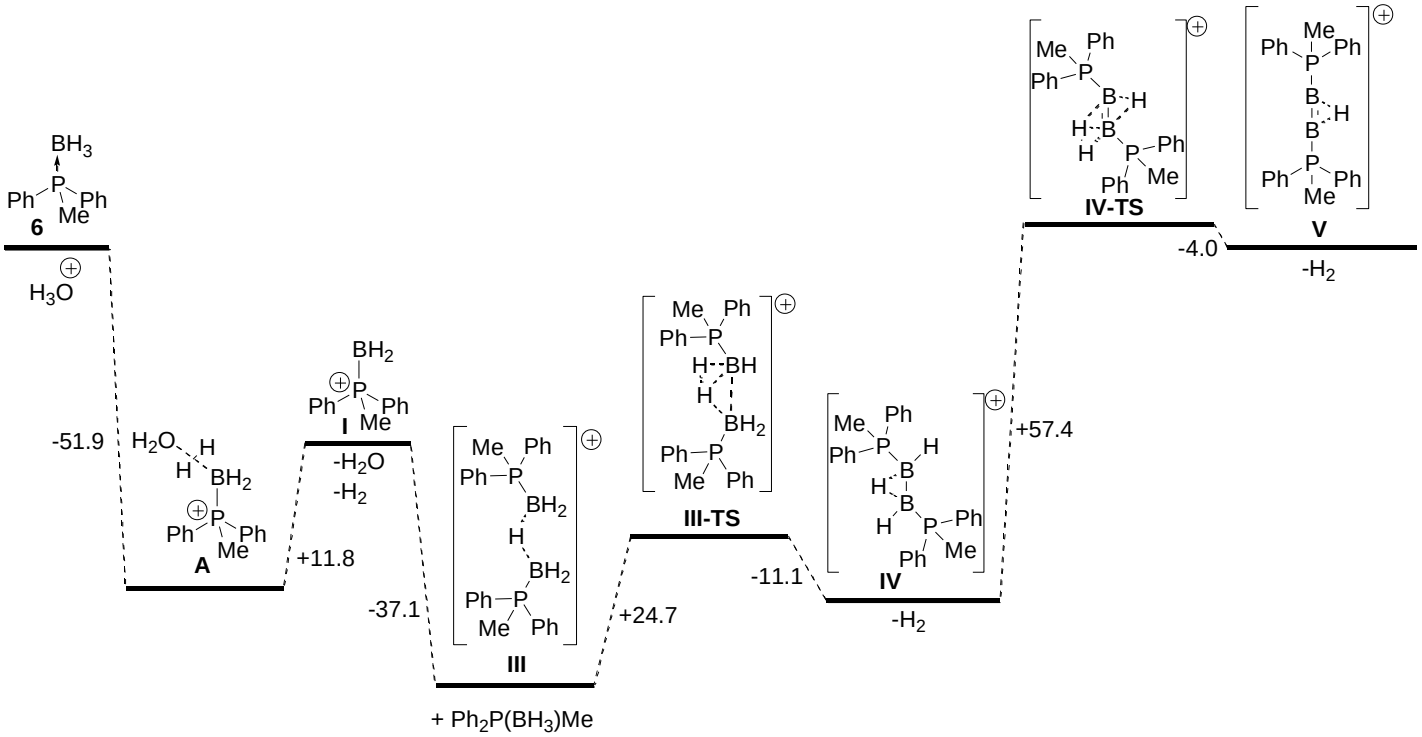

Scheme 2. DFT analysis of the transformation of **6**.

It has been assumed that the first step is the reaction of phosphine–borane **6** with H_3O^+. This reaction should involve the hydrogen atom bonded to boron since the most negative electrostatic potential in the molecule is found there according to DFT calculations (Figure 3a), as indicated by blue translucent spheres surrounding hydrogen atoms. The reaction between **6** and H_3O^+ proceeds without any activation barrier, leading to the adduct **A**. This intermediate undergoes water and hydrogen elimination which leads to the formation of cation **I** with only slight increase of energy. In the next step, the formation of dimer **III** occurs through a reaction of cation **I** with phosphine–borane **6**. The formation of this intermediate is very favorable, as judged from the remarkable stabilization of the system.

The most positive electrostatic potential in **III** is placed around positively charged phosphorus atoms (red color), and is mostly concentrated around the part found around B–H–B bridge. The stability of the dimeric cation is also evident from HOMO analysis in which the orbital involving B–H bonds can be found at HOMO–8 level (Figure 3b).

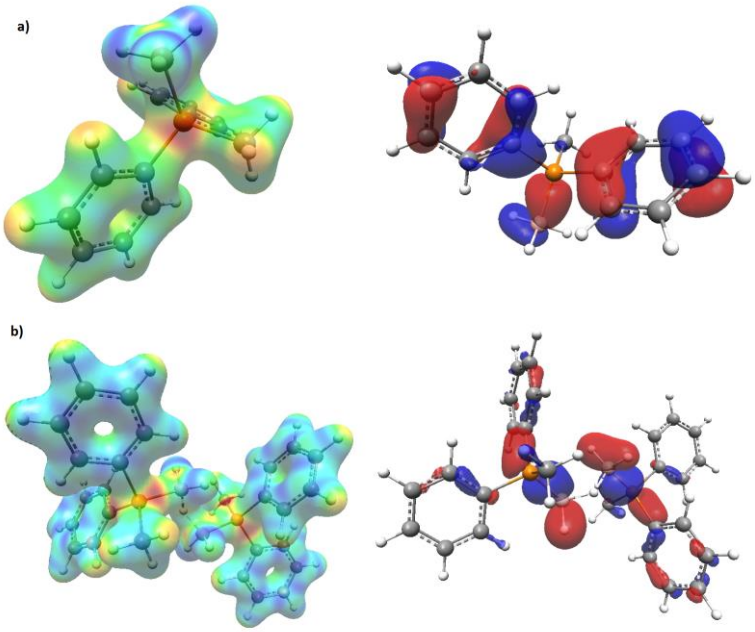

Figure 3. (a) Electrostatic potential map and HOMO orbital for phosphine–borane **6**. (b) Electrostatic potential map and HOMO–8 orbital for intermediate **III**.

Further transformation of the cation **III** might involve hydrogen elimination, which proceeds through transition state **III**–**TS** in which partial formations of hydrogen–hydrogen and boron–boron bonds are present. The activation energy for this step is relatively low (+24.7 kcal/mol), and the potential stabilization of the active complex would include hydrogen elimination, and the formation of intermediate **IV**, with the overall stabilization of –11.1 kcal/mol (Scheme 2). The structure of the intermediate **IV** reveals the presence of an increased negative potential between two boron atoms, which is also reflected by the presence of the HOMO orbital involving boron atoms and B–H–B bridge (Figure 4a).

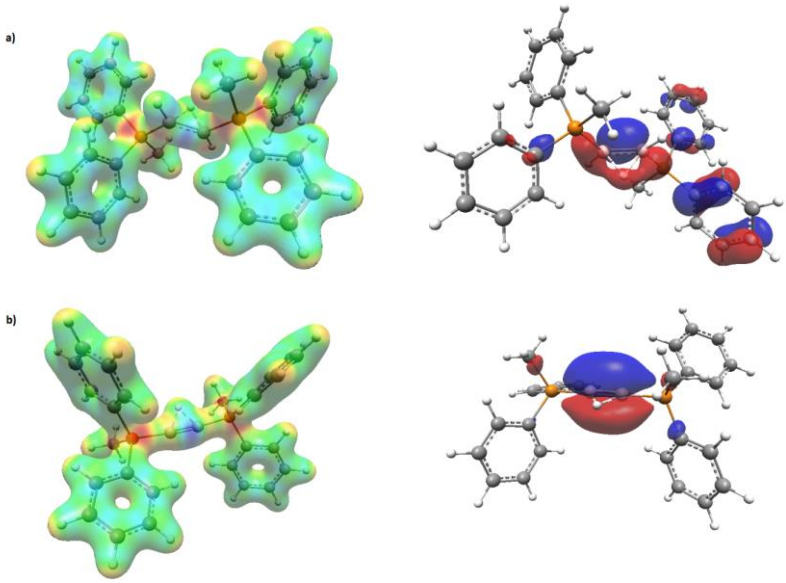

Figure 4. (a) Electrostatic potential map and HOMO orbital for intermediate **IV**. (b) Electrostatic potential map and HOMO orbital for intermediate **V**.

Transformation of intermediate **IV** includes the loss of the second hydrogen molecule, and proceeds through transition state **IV**–**TS** where formation of the hydrogen–hydrogen bond is found along with shortening of the boron–boron bond, and formation of another B–H–B bridge. This process, however, requires a relatively high activation energy (+57.4 kcal/mol), and affords the final intermediate **V**, with slight stabilization (–4.0 kcal/mol).

The formation of dication **II** is proposed to proceed via a different mechanism as shown in Scheme 3.

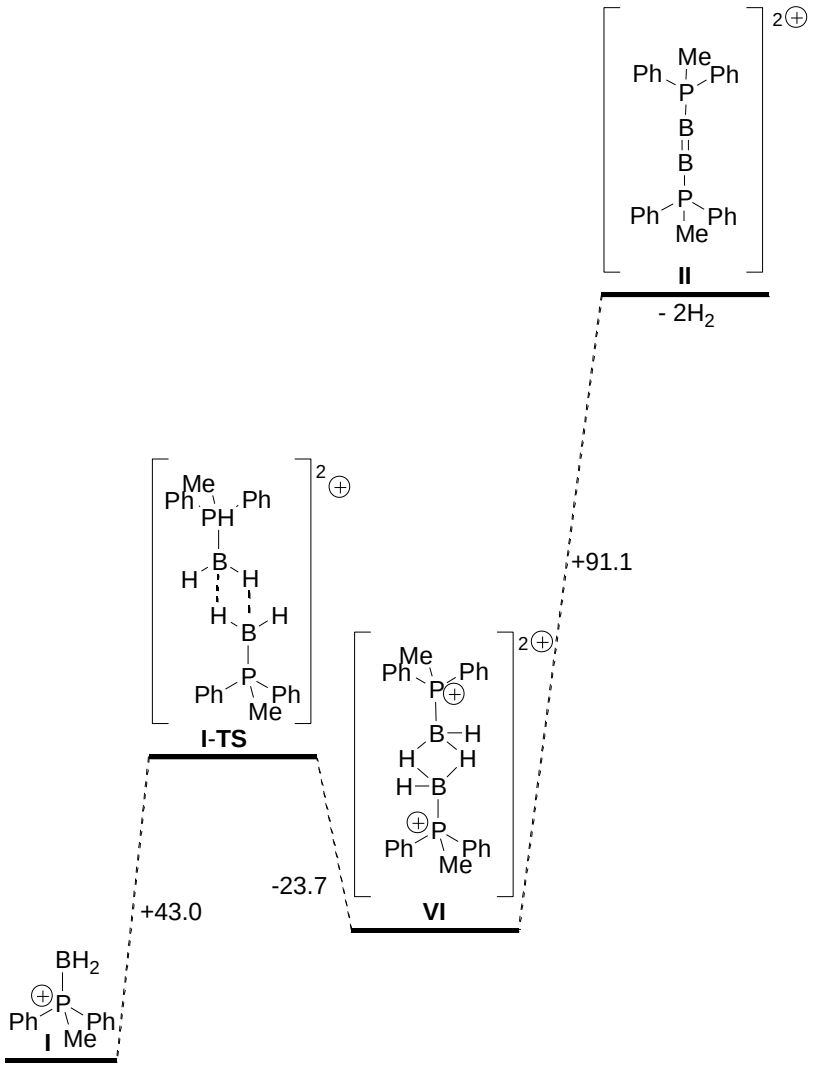

Scheme 3. DFT analysis of the formation of **II**.

In this case, dimerization of cation **I** should proceed through the transition state **I**–**TS** in which the formation of a four–membered B–H–B–H– ring is the crucial step. The activation energy for this transformation was found to be +43.0 kcal/mol which leads to the cyclic dication **VI** with –23.7 kcal/mol of overall stabilization. Dication **VI** resembles the structure typical for boranes, especially for the diborane B_2H_6, the structure of which has been definitively proved by Hedberg and Schomaker.[7] This dication undergoes a concerted process in which two hydrogen molecules are cleaved from the dication leading to the final dication **II**. This process was found to proceed without any activation barrier, as dissociation of two hydrogen molecules from **VI** occurs with a steady destabilization of the system. Overall, this process is highly energy demanding (+91.1 kcal/mol) which can explain a generally low intensity of these mass peaks. The same

process could potentially occur via step-wise elimination of hydrogen molecules. In this case, however, a mass peak around *m/z* 212 should be detected, as the formation of this dication should occur more readily than dication **II**. The lack of mass peak *m/z* 212 has been attributed to a synchronous elimination of two H_2 molecules from **VI**.

The behavior discussed for phosphine–borane **6** reflects, to some extent, the behavior of other compounds possessing dative phosphorus–boron bonds. The data of RP–HPLC–HRMS analyses of compounds **1**–**30** are presented in Table 1.

Table 1. Mass peak distribution for phosphine–boranes **1**–**30**. Letters in parentheses describe the signals as follow: s – strong, m – medium, w – weak

Compound	Parent mass peaks				
	$[M-H]^+$	$[2M-H]^+$	$[2M-3H]^+$	$[2M-5H]^+$	$[2M-6H]^{2+}$
1	229.0944				
2	151.0836 (w)	303.1765 (w)	-	-	149.0677 (w)
3	227.0875 (w)	455.1949 (s)	-	-	225.0763 (w)
4	241.1110 (w)	483.2356 (s)	-	-	239.0923 (w)
5	-	511.2596 (s)	-	-	253.1087 (w)
6	213.1001 (w)	427.2068 (s)	425.1928 (w)	423.1760 (s)	211.0846 (w)
7	227.1153 (w)	455.2381 (s)	-	-	225.1013 (w)
8	275.0928 (s)	551.1958 (w)	-	-	-
9	289.1052 (w)	579.2243 (s)	-	-	287.0924 (w)
10	303.1239 (w)	607.2565 (s)	605.2406 (w)		301.1075 (w)
11	-	635.2866 (s)	633.2671 (w)	-	315.1229 (w)
12	-	663.3150 (s)	-	-	329.1391 (w)
13	253.1303 (w)	507.2690 (s)	-	-	251.1154 (w)
14	-	535.2993 (s)	533.2852 (w)	531.2725 (w)	265.1263 (w)
15	-	563.3327 (s)	561.3182 (w)	559.3009 (w)	279.1477 (w)
16	-	591.3649 (s)	-	-	293.1628 (w)
17	245.0708 (s)	-	489.1395 (w)	-	243.0602 (w)
18	317.1282 (s)	-	-	-	-
19	318.1570 (s)	-	-	-	-
20	195.1096 (s)	-	-	-	193.0941 (s)
21	209.1252 (s)	-	-	-	207.1095 (w)
22	-	355.2090 (m)	-	351.1749 (w)	175.0835 (w)
23	-	-	-	-	189.0997 (w)
24	425.1924 (m)		421.1608 (m) $[M-5H]^+$		
25	439.2074 (m)		435.1757 (s) $[M-5H]^+$		
26	329.2238 (s)	-	-	-	327.2076 (w)
27	329.1253 (s)	-	-	-	-
28	331.1412 (w)	-	-	-	-
29	265.1516 (s)	-	-	-	-
30	365.1457 (w)	-	-	-	-

For secondary phosphine–borane **1**, HRMS analysis showed the presence of only one $[M–H]^+$ mass peak. Phosphine–boranes **2** and **7** transform into $[M–H]^+$, $[2M–H]^+$ and $[2M–6H]^{2+}$ cations with $[2M–H]^+$ being the most abundant one. Phosphine–boranes **3**–**5** and **8**–**12**, with haloalkyl substituents at the phosphorus, generally follow the same pattern, except for compounds with longer alkyl linker where $[M–H]^+$ cations were absent. Cycloalkylphosphine–boranes **13**–**16** underwent ionization mainly with the formation of $[2M–H]^+$, $[2M–3H]^+$, $[2M–5H]^+$ and $[2M–6H]^{2+}$ cations, but phosphine–boranes **17**–**22** and **26**, possessing additional heteroatoms in the structure, underwent ionization predominantly into $[M–H]^+$ cations with only a small population of $[2M–6H]^{2+}$ species. Phosphine–boranes **27**–**30** behaved even more straightforward, leading, exclusively, to $[M–H]^+$ cations.

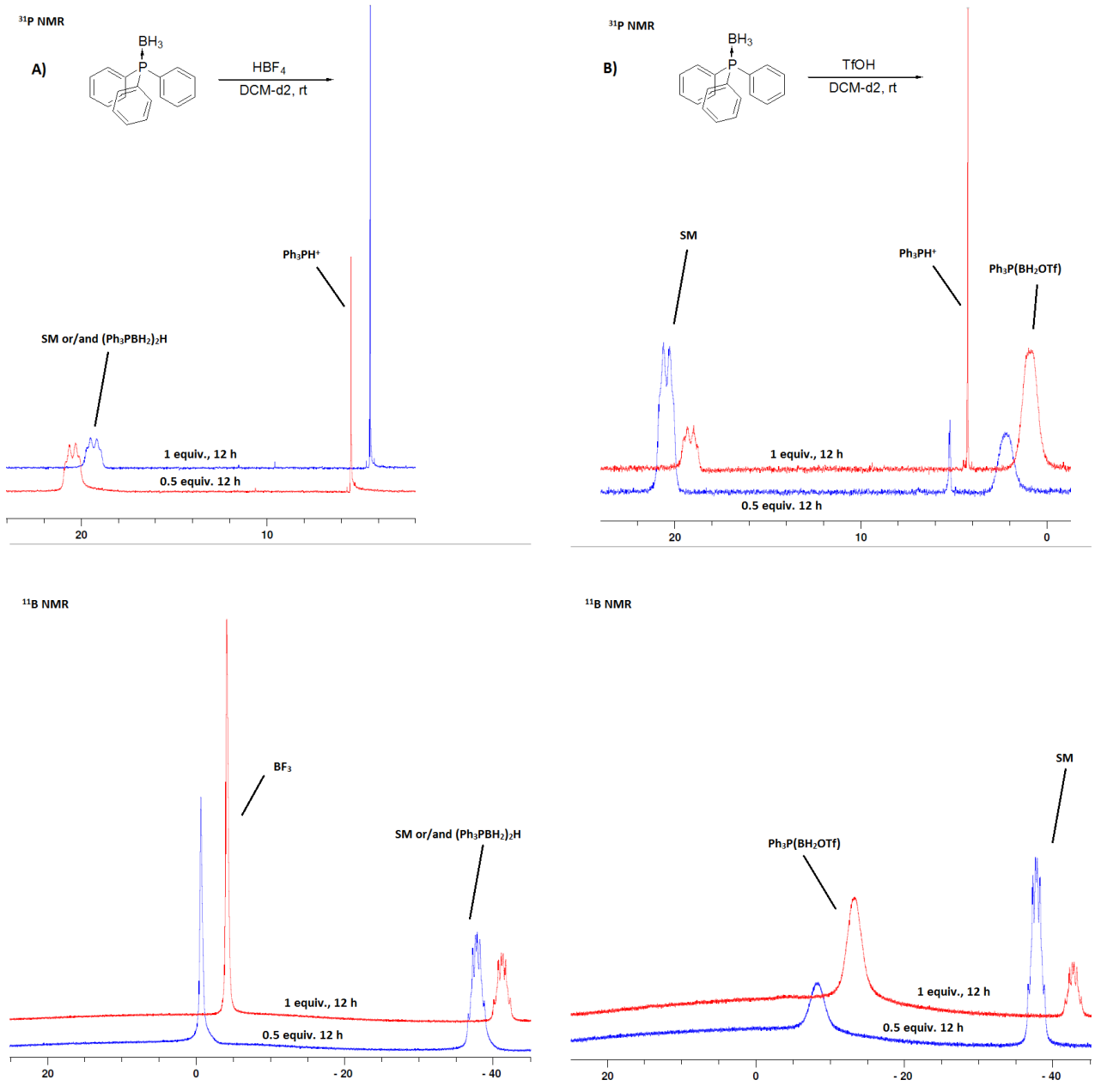

Figure 5. ^{31}P and ^{11}B NMR analyses of the reactions of **34** with different concentrations of strong acids HBF_4 and TfOH.

The ease of formation of $[M–H]^+$ and $[2M–H]^+$ cations raised the question of whether these species could be obtained under milder or even standard conditions. It is known that liberation of free phosphines from their borane complexes can be achieved by a reaction with a strong acid, especially for electronically-rich phosphines.[8,9] In this case, however, at least a 5-fold excess has been used to assure complete transformation of phosphine–borane into free phosphine. It was, therefore, decided to check the reactivity of stoichiometric amounts of strong acids towards a model phosphine–borane.

NMR experiments were performed using the triphenylphosphine–borane **34** which was subjected to a reaction with two strong acids, HBF_4 and TfOH, in two different stoichiometries (0.5 and 1 equiv.) (Figure 5).

Addition of either 0.5 or 1 equivalent of HBF_4 to a solution of $Ph_3P(BH_3)$ **34** in DCM–d_2 led to a vigorous evolution of gas which ceased shortly thereafter. ^{31}P NMR spectra of the reaction mixture performed after mixing showed the presence of two signals at 20.5 ppm (major) and 5.5 ppm (minor), respectively. The same signals (but at a different rate) were observed in the spectrum obtained 12 h later (Figure 5A, top). The first could be attributed to the substrate, however, hydrogen evolution at the beginning of the reaction led to a conclusion that the formation of $Ph_3P–BH_2$, followed by an immediate formation of $[Ph_3P–BH_2–H–BH_2–PPh_3]^+$, should occur under the reaction conditions. Therefore, it should be assumed that the signal in the ^{31}P NMR corresponding to the cationic dimer should appear in the same region as substrate, which is the consequence of a bridgehead hydrogen atom present in the dimeric cation.

Apart from this signal, the presence of a peak at 5.5 ppm was observed in the ^{31}P NMR spectrum of the reaction mixture which evolved over time. This signal has been ascribed to Ph_3PH^+ cation according to the literature.[10] In the ^{1}H NMR, a signal at 8.70 ppm was found with $J_{P–H}$ 520.8 Hz, which supports the structure of this cation. In the ^{11}B NMR, the presence of two signals at –0.7 ppm and –37.7 ppm (multiplet), respectively, was detected (Figure 5A, bottom). The first signal may be assigned to BF_3 or $BF_4^–$ derived from HBF_4. The multiplet at –37.7 ppm should be, in consequence, ascribed to both the substrate and cationic species $[Ph_3P–BH_2–H–BH_2–PPh_3]^+$.

A reaction of either 0.5 or 1 equivalent of TfOH with $Ph_3P(BH_3)$ **34** in DCM–d_2 proceeded in a similar manner, affording a mixture of compounds (Figure 5B). ^{31}P NMR spectra of the reaction mixture recorded after mixing showed the presence of three signals at 20.5 ppm, 5.5 ppm, and 2.3 ppm, respectively. The same signals (but at a different rate) were observed in the spectrum obtained 12 h later (Figure 5B, top). Signals at 20.5 ppm and 2.3 ppm were both broad which suggests the presence of P–B bond in the molecule. Signals at 20.5 ppm and 5.5 ppm were also present in the reaction of **34** with HBF_4, while the signal at 2.3 ppm appeared as a new peak. This signal corresponds most probably to the $Ph_3P–BH_2OTf$ molecule as a reaction between **34** and TfOH proceeded with vigorous evolution of hydrogen, generating a $Ph_3P–BH_2$ cation which undergoes immediate coordination to the triflate anion. The same trend in chemical shift was observed when trimethylphosphine–borane (–1.8 ppm)[11] was allowed to react with methanesulfonic acid (MsOH), affording $Me_3P–BH_2OMs$ (–13.9 ppm).[12] In the ^{11}B NMR, the presence of two signals at –8.4 ppm and –37.7 ppm (multiplet), respectively, was detected (Figure 5B, bottom). The first signal may be assigned to $Ph_3P–BH_2OTf$, whereas, the multiplet at –37.7 ppm belongs to the substrate. The presence of the cationic species $[Ph_3P–BH_2–H–BH_2–PPh_3]^+$ was deemed probable, but not definitive, as it gives the same shift in the ^{11}B NMR spectrum.

Interesting cases were the diphosphine–diboranes **24** and **25** which underwent transformation into $[M–H]^+$ and $[M–5H]^+$–type cations. It seems that the formation of the $[M–H]^+$ species might be favorable in this case due to the formation of ethe 7–membered cyclic structure for **24** (**24a**), and 8–membered cyclic structure for **25** (**25a**) (Figure 6).

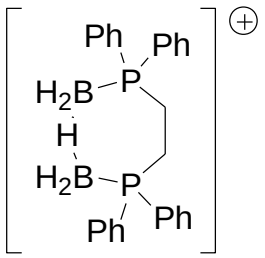

24a

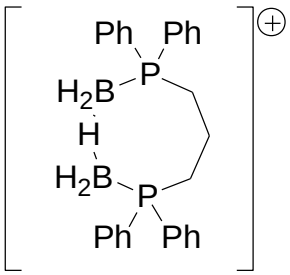

25a

Figure 6. Monocations derived from **24** and **25**.

Organophosphorus compounds of $R_3P–BH_3$ and $R_2P–BH_2$ types can be regarded as borohydride and borane analogues, at least theoretically. In organic synthesis, $NaBH_4$ and BH_3 are often reagents of choice for reduction of carbon–heteroatom double bonds. Compounds of $R_2P–BH_2$ type possess quite interesting properties as they can be regarded both as Lewis base and Lewis acid due to the presence of a free-electron pair (at phosphorus) and electron vacancy (at boron). As a consequence, they readily undergo oligomerization[13,14] and cyclooligomerization[15-17] reactions, affording products with multiple –P–B– linkage. When considering reducing properties of either $R_3P–BH_3$ or $R_2P–BH_2$ type compounds, the only mention found in the literature was either intermolecular[18] or intramolecular[19-21] hydroboration of a C=C bond with $R_3P–BH_3$ type compounds. A combination of these molecules, i.e., $R_3P–BH_3$ or $R_2P–BH_2$, however, can serve as a system for reduction of multiple bonds in which the $P–BH_2$ fragment activates multiple bonds and $R_3P–BH_3$ provides a hydride anion (Figure 7).

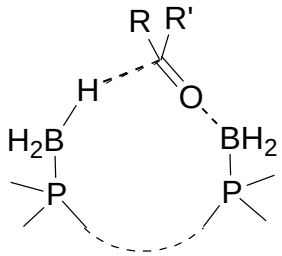

Figure 7. Diborane monocations as potential reducing agents.

The best model reaction to test the hypothesis stated above is the reduction of the C=O bond, as boron forms a strong dative bond with the carbonyl oxygen, thus, activating the carbonyl group and facilitating a hydride transfer from the second boron functionality. For a test reaction, acetophenone has been used as the model carbonyl compound which was then reacted with a monocation derived from the diphosphine–diborane **24** and TfOH (Scheme 4).

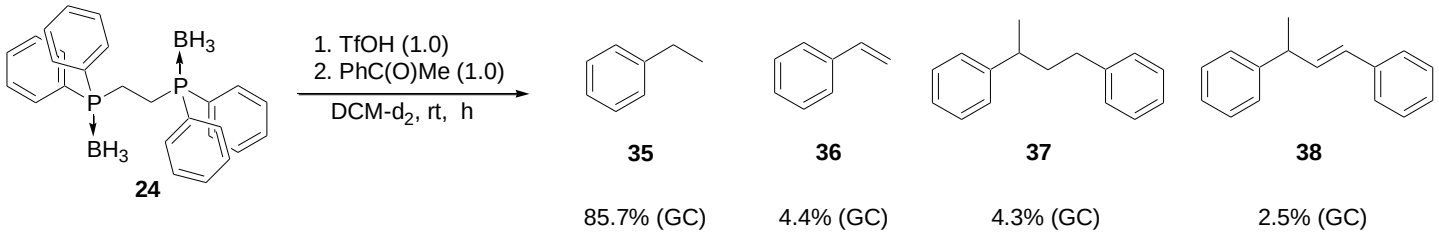

Scheme 4. Attempted reduction of acetophenone with monocation derived from **24**.

The reaction was performed in a NMR tube using stoichiometric amounts of reagents; the progress of the reaction was followed by ^{1}H, ^{31}P and ^{11}B NMR analyses as shown below (Figure 8).

The ^{1}H NMR spectrum, recorded after 30 min, revealed the presence of two major compounds: acetophenone and ethylbenzene **35** in 0.41:1.00 ratio. Apart from these two compounds, traces of styrene were detected in the olefinic region. The presence of a minor amount of DPPE diborane (singlet at 2.44 ppm) and major amount of $Ph_2P(BH_3)CH_2CH_2P(BH_2OTf)Ph_2$ (multiplets at 2.43-2.71 ppm) have been confirmed as well. Additionally, other multiplets in the 2.73-3.46 ppm region started to appear, which could be ascribed to the products of the DPPE-diborane transformation. During the time, the amount of acetophenone constantly decreased with a simultaneous increase of the amount of ethylbenzene.

In the ^{31}P NMR spectra, the initial shifts of $Ph_2P(BH_3)CH_2CH_2P(BH_2OTf)Ph_2$ were at 18.5 and 0.7 ppm, respectively. After 30 minutes, additional signals at 9.4 ppm (J_{P-P} 52 Hz), 10.5 (singlet) and 26.9 ppm (broad multiplet), respectively, were found. The intensity of the latter increased over time with simultaneous decrease in the intensity of the signals of the parent compound. The presence of the doublet at 9.4 ppm with a relatively large coupling constant suggests the formation of a cationic intermediate with the possible structure like $Ph_2P(BH_3)CH_2CH_2P(H)Ph_2$, and the signal at 10.5 ppm might correspond to the dicationic $Ph_2P(H)CH_2CH_2P(H)Ph_2$.

In the ^{11}B NMR, the signals of the initial $Ph_2P(BH_3)CH_2CH_2P(BH_2OTf)Ph_2$ appear at -40.4 ppm and -9.3 ppm, respectively. Apart from this, a characteristic and very broad peak around 0 ppm appeared, corresponding to B_2O_3 oxide, along with a peak at -34.5 ppm. The latter corresponds to a phosphine-borane different from the substrate. Over time, the intensity of the signals of the starting borane decreased with a steady increase of a broad B_2O_3 signal.

A detailed analysis of the reaction mixture revealed one surprising observation which was the lack of the most obvious reduction product, 1-phenylethanol. Instead, ethylbenzene is the major reaction product as deduced from NMR and GC-MS analysis, formed in almost 86% yield. In this regard, the reaction could be regarded as a hydrodeoxygenation, but the presence of trace amounts of styrene points toward a more complex mechanism. This most probably involves reduction of acetophenone to 1-phenylethanol, followed by its dehydration to styrene. The latter most likely undergoes hydroboration of the double bond, followed by hydrolysis of the boron-oxygen bond with water formed in the previous step.

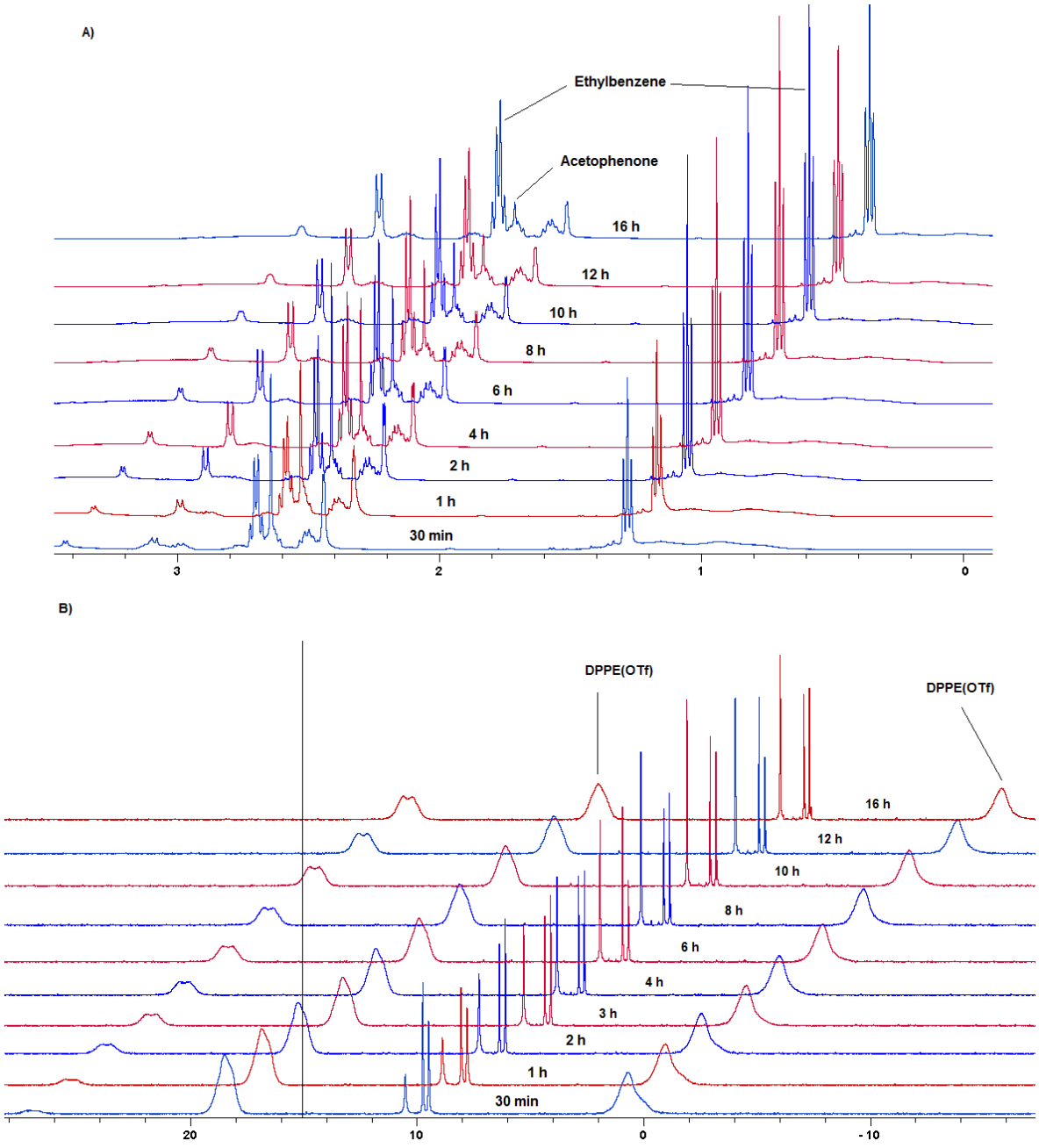

Figure 8. Monitoring of a reaction of acetophenone with $Ph_2P(BH_3)CH_2CH_2P(BH_2OTf)Ph_2$, formed from DPPE diborane and TfOH, followed by (a) ^{1}H NMR and (b) ^{31}P NMR.

This reaction is quite unique, as, in general, the transformation of aryl alkyl ketones into the appropriate alkylarenes requires either strong reducing agents[22-24] or use of the appropriate catalyst.[25-28] Borane complexes used for reduction of aryl alkyl ketones generally provide the appropriate secondary alcohols.[29-32] In this case, activated phosphine-borane affords alkylarene under very mild reaction conditions. The scope of this transformation is currently underway in our laboratory.

Conclusions

A set of phosphine–boranes has been subjected to RP–HPLC–HRMS analysis using reverse-phase chromatography coupled to an IT–TOF mass spectrometer. All of the phosphine–boranes underwent a formal hydride-anion cleavage, affording $[M–H]^+$ cations as the primary mass peaks. In some cases, the initial $[M–H]^+$ cations underwent further transformations, affording $[2M–H]^+$, $[2M–3H]^+$, $[2M–5H]^+$ or $[2M–6H]^{2+}$ type species under the measurement conditions. The formation of all detected mass peaks is a consequence of a reaction of phosphine–boranes with a proton source in which the organophosphorus compound serves as a hydride donor. The formation of other mass peaks can be inferred on the basis of the reaction of the $[M–H]^+$ cation with the starting phosphine–borane followed by further hydrogen molecule cleavage. The enormous stability of the $[2M–H]^+$ cation has been proven by using a reaction between $R_3P–BH_3$ and a strong acid monitored by ^{31}P and ^{11}B NMR spectroscopies. A detailed analysis of their structures has led to the conclusion that these species might act as carbonyl-group activators. . It has been shown that activated phosphine-boranes are able to react with ketones, however, instead of simple C=O bond reduction, the formation of deoxygenated products was observed which suggests more complex behavior of these cationic species. Further investigations are currently underway.

Experimental Section

General. All reactions were performed under an argon atmosphere using Schlenk techniques. Only dry solvents were used, and the glassware was heated under vacuum prior to use. Solvents for chromatography were distilled once before use, and solvents for extraction were used as received. Tetrahydrofurane was dried over sodium/benzophenone ketyl.

NMR spectra were recorded with Bruker Ascend 500 MHz spectrometer in $CDCl_3$ as a solvent at room temperature unless otherwise noted. Chemical shifts (δ ppm) are reported relative to the residual- solvent peak. NMR Data analysis has been performed using the software provided by the supplier. Melting points were measured using Büchi M-560 and were uncorrected. GC–MS analysis was performed using a Shimadzu GC–2010 gas chromatograph coupled with Shimadzu GCMS–QP2010S mass spectrometer. Mass spectra were recorded in electron ionization (EI, 70 eV) mode with a standard column using the following parameters: pressure 65kPa, total flow 33.9 mL/min, column flow 1.0 mL/min, linear velocity 36.8 cm/s, split 30, temperature program (80 °C hold 0.5 min, 80–340 °C/19 °C/min hold 2 min, 300–340 °C/15 °C/min hold 3.26 min total 20 min). MS Data analysis has been performed using the software provided by the supplier. High resolution mass spectrometry analyses were obtained using a Shimadzu LCMS–IT–TOF mass spectrometer, coupled with Shimadzu UFLC XR system (LC–20AD XR pumps, SPD–20A detector, SIL–20AC XR autosampler), working in a reverse-phase system. The LCMS–IT–TOF system was equipped in electrospray (ESI) ionization mode, and the formed ions were analyzed using an IT trap followed by TOF analyzer. Data were collected using both positive and negative modes. HRMS Data analysis has been performed using the software provided by the supplier. Thin layer chromatography (TLC) was performed with precoated silica gel plates and visualized by UV light or iodide on silica gel. The reaction mixtures were purified by column chromatography over silica gel (60−240 mesh).

Compounds **1**,[33] **2**,[34] **6**,[35] **3-5** and **8-12**,[36] **7**,[37] **13-16**,[37] **17-19** and **27**,[38] **22**,[39] **23**,[37] **25**[39] and **26**[37] were obtained by literature procedures.

The synthesis of 20 and 21. In a flame–dried Schlenk tube (25 mL) equipped with magnetic stirrer and argon inlet dimethylphenylphosphine–borane **2** (0.151 g, 1 mmol) was dissolved in dry degassed THF (5 mL). After cooling to −78 °C a solution of *n*–BuLi (0.94 mL, 1.6 M in hexanes, 1.5 mmol) was added and the mixture was stirred at −78 °C for 1 h. Then, ethylene (0.6 mL, 2.5 M in THF, 1.5 mmol) or (*R*)–propylene oxide (0.105 mL, 1.5 mmol) was added, the cooling bath removed and the mixture was stirred for 2 h. The reaction was quenched with saturated aq. NH_4Cl solution, the aqueous layer was extracted with DCM (3x12 mL), the combined organic fractions were dried over $MgSO_4$, filtered, and evaporated under reduced pressure. The residue was purified by column chromatography using hexane/ethyl acetate 6:1 as eluent.

(3–Hydroxypropyl)methylphenylphosphine–borane (20). Isolated as a pale yellow oil, 0.168 g (86%). Rf 0.39 (Hexane:EtOAc 2:1); ^{1}H NMR (500 MHz, $CDCl_3$) δ 7.68–7.78 (m, 2H), 7.43–7.56 (m, 3H), 3.59–3.70 (m, 2H), 2.61 (bs, 1H), 1.88–2.03 (m, 2H), 1.70–1.82 (m, 1H), 1.60–1.70 (m, 1H), 1.58 (d, *J* 10.4 Hz, 3H), 0.38–1.09 (bm, 3H); ^{13}C NMR (126 MHz, $CDCl_3$) δ 131.4 (d, *J* 9.1 Hz), 131.3 (d, *J* 2.7 Hz), 129.5 (d, *J* 53.6 Hz), 128.8 (d, *J* 10.0 Hz), 62.7 (d, *J* 13.6 Hz), 26.1, 23.8 (d, *J* 37.2 Hz), 11.0 (d, *J* 39.1 Hz); ^{31}P NMR (202 MHz, $CDCl_3$) δ 9.2 (bm); GC t_R 9.36 min; GC–MS (EI, 70 eV) *m/z* 182 (M–BH_3) (4), 139 (15), 138 (100), 124 (14), 123 (63), 121 (35), 109 (29), 108 (9), 107 (14), 91 (97), 79 (10), 77 (15), 45 (9); HRMS (ESI–TOF) *m/z*: $[M–H]^+$ Calcd for $C_{10}H_{17}BOP$ 195.1110; Found 195.1096.

(3*R*–3–Hydroxybutyl)methylphenylphosphine–borane (21). Isolated as an equimolar mixture of diastereomers, 0.116 g (55%). Rf 0.52 (Hexane:EtOAc 2:1); ^{1}H NMR (500 MHz, $CDCl_3$) δ 7.69–7.77 (m, 4H), 7.44–7.55 (m, 6H), 3.73–386 (m, 2H), 2.00–2.16 (m, 2H), 1.80–1.94 (m, 2H), 1.50–1.73 (m, 3H), 1.57 (d, *J* 10.4 Hz, 6H), 1.35–1.48 (m, 1H), 1.18 (d, *J* 6.3 Hz, 3H), 1.17 (d, *J* 6.0 Hz, 3H), 0.38–1.08 (bm, 6H); ^{13}C NMR (126 MHz, $CDCl_3$) δ 131.43 (d, *J* 9.1 Hz), 131.37 (d, *J* 8.2 Hz), 131.28 (d, *J* 2.7 Hz), 129.6 (d, *J* 53.6 Hz), 129.3 (d, *J* 53.6 Hz), 128.8 (d, *J* 9.1 Hz), 68.0 (d, *J* 11.8 Hz), 32.1 (d, *J* 1.8 Hz), 23.6 (d, *J* 1.8 Hz), 23.3, 11.1 (d, *J* 39.1 Hz), 10.8 (d, *J* 39.1 Hz); ^{31}P NMR (202 MHz, $CDCl_3$) δ 9.2 (bm); GC t_R 9.22 min; GC–MS (EI, 70 eV) *m/z* 197 (5), 196 (M–BH_3) (6), 139 (14), 138 (100), 135 (11), 124 (13), 123 (51), 121 (24), 109 (16), 107 (11), 91 (73), 78 (12), 77 (13), 45 (12); HRMS (ESI–TOF) *m/z*: $[M–H]^+$ Calcd for $C_{11}H_{19}BOP$ 209.1267; Found 209.1252.

Synthesis of 27. In a flame–dried Schlenk tube (25 mL) equipped with magnetic stirrer and argon inlet 1–indanone **31** (0.12 g, 0.91 mmol) was placed followed by addition of THF (5 mL). Once 1–indanone was dissolved, the reaction flask was immersed in acetone–dry ice mixture. After 5 min, *n*–BuLi (0.65 mL, 1.4 M in cyclohexane) was added and the mixture was left at −78 °C for an hour. Then, Ph_2PCl (0.163 mL, 0.91 mmol) was added at once and the mixture was allowed to warm to room temperature for an hour. Next, BH_3–THF (1.36 mL, 1.36 mmol, 1 M in THF) was added and the mixture was left for 30 min. The reaction was quenched with saturated aq. NH_4Cl solution, the aqueous layer was extracted with DCM (3x15 mL), the combined organic fractions were dried over $MgSO_4$, filtered, and evaporated under reduced pressure. The residue was purified by column chromatography using hexane/ethyl acetate 6:1 as eluent affording 2–(diphenylboranatophosphinyl)–1–indanone **27** (0.196 g, 65%) as a white solid. mp 143.5–144.6 °C; Rf 0.73 (Hexane:EtOAc 2:1); ^{1}H NMR (500 MHz, $CDCl_3$) δ 7.81–7.87 (m, 2H), 7.74–7.79 (m, 2H), 7.69–7.72 (m, 1H), 7.45–7.59 (m, 5H), 7.34–7.43 (m, 4H), 3.84–3.91 (m, 1H), 3.30–3.48 (m, 2H), 0.46–1.34 (bm, 3H); ^{13}C NMR (126 MHz, $CDCl_3$) δ 200.6, 152.8, 137.0, 135.1, 133.3 (d, *J* 9.1 Hz), 132.6 (d, *J* 9.1 Hz), 131.6, 131.5, 130.9 (d, *J* 10.9 Hz), 128.9 (d, *J* 10.0 Hz), 128.5 (d, *J* 10.0 Hz), 127.8, 126.7 (d, *J* 54.5 Hz), 126.2, 124.1, 42.8 (d, *J* 30.9 Hz), 30.0; ^{31}P NMR (202 MHz, $CDCl_3$) δ 25.1 (bm); HRMS (ESI–TOF) *m/z*: $[M–H]^+$ Calcd for $C_{21}H_{19}BOP$ 329.1267; Found 329.1253.

Synthesis of 28. In a flame–dried Schlenk tube (25 mL) equipped with magnetic stirrer and argon inlet 2–(diphenylboranatophosphinyl)–1–indanone **27** (0.515 g, 1.56 mmol) was placed followed by addition of MeOH (10 mL). Once **27** was dissolved, the reaction flask was immersed in water–dry ice mixture and $NaBH_4$

(0.472g, 12.48 mmol) was added portionwise to avoid excessive evolution of gas. After all $NaBH_4$ was added, the mixture was left at 0 °C for an hour. Then, the mixture was evaporated to dryness and the residue was treated with water (20 mL) and extracted with DCM (3x10 mL). Combined organic fractions were dried over $MgSO_4$, filtered, and evaporated under reduced pressure. The residue was purified by column chromatography using hexane/ethyl acetate 2:1 as eluent affording 2–(diphenylboranatophosphinyl)–1–indanol **28** (0.430 g, 83%) as a white solid. mp 79.9–81.8 °C; Rf 0.78 (Hexane:EtOAc 2:1); ^{1}H NMR (500 MHz, $CDCl_3$) δ 7.87–7.92 (m, 2H), 7.76–7.81 (m, 2H), 7.40–7.57 (m, 8H), 7.27–7.32 (m, 1H), 7.22–7.26 (m, 1H), 5.44–5.47 (m, 1H), 3.46–3.56 (m, 2H), 2.98–3.06 (m, 1H), 2.94 (bs, 1H); ^{13}C NMR (126 MHz, $CDCl_3$) δ 143.3 (d, *J* 4.5 Hz), 141.7 (d, *J* 10.0 Hz), 132.7 (d, *J* 8.2 Hz), 132.5 (d, *J* 9.1 Hz), 131.3, 131.1, 129.3 (d, *J* 3.6 Hz), 129.1, 128.82 (d, *J* 8.2 Hz), 128.76 (d, *J* 7.3 Hz), 127.4, 124.9, 124.6, 76.9, 41.3 (d, *J* 37.2 Hz), 33.0; ^{31}P NMR (202 MHz, $CDCl_3$) δ 16.1 (bm); HRMS (ESI–TOF) *m/z*: $[M–H]^+$ Calcd for $C_{21}H_{21}BOP$ 331.1423; Found 331.1412.

Synthesis of 29. In a flame–dried Schlenk tube (25 mL) equipped with magnetic stirrer and argon inlet *t*–butylphenylphosphine–borane **32** (0.391 g, 2.17 mmol) was placed followed by an addition of THF (10 mL). After all **32** was dissolved, the mixture was cooled to −78 °C and *n*–BuLi (1.63 mL, 2.61 mmol, 1.6 M in hexanes) was added dropwise. After 1 h, ethyl chloroacetate (0.236 mL, 4.34 mmol) was added at the same temperature and the mixture was allowed to warm to room temperature and stir for 4 h. The reaction was quenched with saturated aq. NH_4Cl solution, the aqueous layer was extracted with DCM (3x15 mL), the combined organic fractions were dried over $MgSO_4$, filtered, and evaporated under reduced pressure. The residue was purified by column chromatography using hexane/ethyl acetate 6:1 as eluent affording ethyl (*t*–butylphenylboranatophosphinyl)acetate **29** (0.342 g, 68%) as a colorless sticky oil. Rf 0.46 (Hexane:EtOAc 6:1); ^{1}H NMR (500 MHz, $CDCl_3$) δ 7.75–7.82 (m, 2H), 7.50–7.56 (m, 1H), 7.44–7.50 (m, 2H), 3.98–4.13 (m, 2H), 3.18–3.26 (m, 1H), 2.98–3.05 (m, 1H), 1.15 (d, *J* 14.5 Hz, 9H), 1.08 (t, *J* 7.3 Hz, 3H), 0.41–1.13 (bm, 3H); ^{13}C NMR (126 MHz, $CDCl_3$) δ 167.2, 133.5 (d, *J* 8.2 Hz), 131.5 (d, *J* 2.7 Hz), 128.1 (d, *J* 10.0 Hz), 125.4 (d, *J* 49.1 Hz), 61.5, 29.9 (d, *J* 30.9 Hz), 27.4 (d, *J* 26.3 Hz), 25.4, 13.8; ^{31}P NMR (202 MHz, $CDCl_3$) δ 32.6 (bm); GC t_R 10.19 min; GC–MS (EI, 70 eV) *m/z* 252 ($M–BH_3$) (11), 196 (31), 179 (10), 153 (12), 150 (25), 125 (35), 123 (17), 122 (55), 121 (10), 118 (100), 109 (24), 108 (11), 107 (15), 90 (44), 79 (11), 78 (24), 77 (12), 57 (90), 47 (23); HRMS (ESI–TOF) *m/z*: $[M–H]^+$ Calcd for $C_{14}H_{23}BO_2P$ 265.1529; Found 265.1516.

Synthesis of 30. In a flame–dried Schlenk tube (25 mL) equipped with magnetic stirrer and argon inlet tri(*p*–anisyl)phosphine **33** (0.510 g, 1.45 mmol) was dissolved in THF (5 mL). Then, BH_3–THF (1.74 mL, 1.74 mmol, 1 M in THF) was added at once and the mixture was left at room temperature for 3 h. Then, the mixture was evaporated to dryness and the residue was treated with water (20mL) and extracted with DCM (3x10 mL). Combined organic fractions were dried over $MgSO_4$, filtered, and evaporated under reduced pressure. The residue was purified by column chromatography using hexane/ethyl acetate 6:1 as eluent affording tri(*p*–anisyl)phosphine–borane **30** (0.530 g, 100%) as a white solid. mp 140.8–141.6 °C; Rf 0.78 (Hexane:EtOAc 6:1); ^{1}H NMR (500 MHz, $CDCl_3$) δ 7.46–7.53 (m, 6H), 6.92–6.97 (m, 6H), 3.84 (s, 9H), 0.89–1.57 (bm, 3H); ^{13}C NMR (126 MHz, $CDCl_3$) δ 161.8, 134.6 (d, *J* 10.9 Hz), 120.8 (d, *J* 62.7 Hz), 114.3 (d, *J* 10.9 Hz), 55.3; ^{31}P NMR (202 MHz, $CDCl_3$) δ 16.4 (bm); GC t_R 20.01 min; GC–MS (EI, 70 eV) *m/z* 353 (21), 352 ($M–BH_3$) (94), 337 (8), 245 (18), 214 (15), 199 (12), 139 (13), 138 (100); HRMS (ESI–TOF) *m/z*: $[M–H]^+$ Calcd for $C_{21}H_{23}BO_3P$ 365.1478; Found 365.1457.

Reaction of 34 with strong acids. In a flame–dried NMR tube triphenylphosphine-borane **34** (0.1 g, 0.362 mmol) was placed followed by addition of DCM-d_2 (0.7 mL). Then, either HBF_4-OEt_2 (0.5 or 1 equiv.) or TfOH (0.5 or 1 equiv.) was added to the tube, the mixture was shaked well and the reaction process was monitored to ^{1}H, ^{11}B and ^{31}P NMR analysis over 12 h period.

Reaction of 24 with acetophenone in the presence of strong acids. In a flame–dried NMR tube DPPE-$(BH_3)_2$ **24** (0.1 g, 0.235 mmol) was placed followed by addition of DCM-d_2 (0.7 mL). Then, acetophenone (0.027 mL, 0.235 mmol) was added followed by strong acid (1 equiv.). The mixture was shaked well and the reaction process was monitored to ^{1}H, ^{11}B and ^{31}P NMR analysis over 16 h period.

Calculations. The theoretical results were obtained with the aid of the density functional theory (DFT) approach.[40] In all reported cases the B3LYP hybrid functional[41] in conjunction with the polarized valence triple zeta (VTZP) basis set 6-311++G**[42,43] augmented with diffuse functions was used. The geometry optimization for all the systems followed by the frequency calculations were performed. The type of a stationary point during optimization procedure was determined based on the analysis of the obtained frequencies. In the case of minima (stable molecules) all computed frequencies were real. One imaginary frequency was obtained in the case of each transition state. All the reported energies were corrected for the zero point vibrational energies (ZPVE). The calculations were carried out using PQS quantum chemistry package.[44]

Acknowledgements

Financial support from National Science Centre (SONATA BIS project 2012/07/E/ST5/00544) is kindly acknowledged.

Supplementary Material

NMR data (^{1}H, ^{13}C and ^{31}P NMR spectra) for all synthesized compounds have been included in a Supplementary Material file associated with this manuscript.

References

1. Brunel, J. M.; Faure, B.; Maffei, M. *Coord. Chem. Rev.* **1998**, *178-180*, 665-698. https://doi.org/10.1016/S0010-8545(98)00072-1
2. Ohff, H.; Holz, J.; Quirmbach, M.; Börner, A. *Synthesis*, **1998**, 1391-1415. https://doi.org/10.1055/s-1998-2166
3. Imamoto, T.; Tamura, K.; Ogura, T.; Ikematsu, Y.; Mayama, D.; Sugiya, M. *Tetrahedron: Asymmetry*, **2010**, *21*, 1522-1528. https://doi.org/10.1016/j.tetasy.2010.03.025
4. Hoge, G.; Wu, H.-P.; Kissel, W. S.; Pflum, D. A; Greene, D. J.; Bao, J. *J. Am. Chem. Soc.*, **2004**, *126*, 5966-5967. https://doi.org/10.1021/ja048496y
5. Tsuruta, H.; Imamoto, T. *Tetrahedron: Asymmetry*, **1999**, *10*, 877-882. https://doi.org/10.1016/S0957-4166(99)00042-7
6. Yamanoi, Y.; Imamoto, T. *J. Org. Chem.*, **1999**, *64*, 2988-2989. https://doi.org/10.1021/jo990131m
7. Hedberg, K.; Schomaker, V. *J. Am. Chem. Soc.*, **1951**, *73*, 1482-1487. https://doi.org/10.1021/ja01148a022

8. Sugama, H.; Saito, H.; Danjo, H. Imamoto, T. *Synthesis*, **2001**, 2348-2353. https://doi.org/10.1055/s-2001-18433
9. Rivard, M.; Guillen, F.; Fiaud, J.-C.; Aroulanda, C.; Lesot, P. *Tetrahedron: Asymmetry*, **2003**, *14*, 1141-1152. https://doi.org/10.1016/S0957-4166(03)00202-7
10. Mann, B. E.; Guzman, M. H. *Inorg. Chim. Acta*, **2002**, *330*, 143-148. https://doi.org/10.1016/S0020-1693(01)00712-5
11. Busacca, C. A.; Raju, R.; Grinberg, N.; Haddad, N.; James-Jones, P.; Lee, H.; Lorenz, J. C.; Saha, A.; Senanayake, C. H. *J. Org. Chem.*, **2008**, *73*, 1524. https://doi.org/10.1021/jo7024064
12. Oshiki, T.; Imamoto, T. *Bull. Chem. Soc. Jpn*, **1990**, *63*, 2846-2849. https://doi.org/10.1246/bcsj.63.2846
13. Rivard, E.; Lough, A. J.; Manners, I. *J. Chem. Soc. Dalton Trans.*, **2002**, 2966-2972. https://doi.org/10.1039/B202361J
14. Denis, J.-M.; Forintos, H.; Szelka, H.; Toupet, L.; Pham, T.-N.; Madec, P.-J.; Gaumont, A.-C. *Chem. Commun.* **2003**, 54-55. https://doi.org/10.1039/B206559B
15. Dorn, H.; Singh, R. A.; Massey, J. A.; Nelson, J. M.; Jaska, C. A.; Lough, A. J.; Manners, I. *J. Am. Chem. Soc.*, **2000**, *122*, 6669-6678. https://doi.org/10.1021/ja000732r
16. Pham-Tran, N.-N.; Huy, N.-H. T.; Nam, P.-C.; Ricard, L.; Nguyen, M. T. *J. Organomet. Chem.*, **2006**, *691*, 4058-4064. https://doi.org/10.1016/j.jorganchem.2006.06.011
17. Burck, S.; Gudat, D.; Nieger, M.; Vinduš, D. *Eur. J. Inorg. Chem.*, **2008**, 704-707. https://doi.org/10.1002/ejic.200700964
18. Pelter, A.; Rosser, R. Mills, S. *J. Chem. Soc., Chem. Commun.*, **1981**, 1014-1015. https://doi.org/10.1039/C39810001014
19. Gaumont, A.-C.; Bourumeau, K.; Denis, J.-M.; Guenot, P. *J. Organomet. Chem.*, **1994**, *484*, 9-12. https://doi.org/10.1016/0022-328X(94)87178-7
20. Scheideman, M.; Shapland, P.; Vedejs, E. *J. Am. Chem. Soc.*, **2003**, *125*, 10502-10503. https://doi.org/10.1021/ja034655m
21. Shapland, P.; Vedejs, E. *J. Org. Chem.*, **2004**, *69*, 4094-4100. https://doi.org/10.1021/jo040125c
22. Eisch, J. J.; Liu, Z.-R.; Boleslawski, M. P. *J. Org. Chem.*, **1992**, *57*, 2143-2147. https://doi.org/10.1021/jo00033a041
23. Olah, G. A.; Arvanaghi, M.; Ohanessian, L. *Synthesis*, **1986**, 770-772. https://doi.org/10.1055/s-1986-31773
24. Hitomi, S.; Reiko, M.; Hirohisa, K.; Atsuhiro, O. *Chem. Lett.*, **1983**, *12*, 909-910. https://doi.org/10.1246/cl.1983.909
25. Mirza-Aghayan, M.; Kalantari, M.; Boukherroub, R. *Appl. Organomet. Chem.*, **2019**, *33*, e4837. https://doi.org/10.1002/aoc.4837
26. Offner-Marko, L.; Bordet, A.; Moos, G.; Tricard, S.; Rengshausen, S.; Chaudret, B.; Luska, K. L.; Leitner, W. *Angew. Chem. Int. Ed.*, **2018**, *57*, 12721-12726. https://doi.org/10.1002/anie.201806638

27. La Sorella, G.; Sperni, L.; Canton, P.; Coletti, L.; Fabris, F.; Strukul, G.; Scarso, A. *J. Org. Chem.*, **2018**, *83*, 7438-7446. https://doi.org/10.1021/acs.joc.8b00314
28. Schäfer, C.; Ellstrom, C. J.; Cho, H.; Török, B. *Green Chem.*, **2017**, *17*, 1230-1234. https://doi.org/10.1039/C6GC03032G
29. Fujioka, H.; Yahata, K.; Kubo, O.; Sawama, Y.; Hamada, T.; Maegawa, T. *Angew. Chem. Int. Ed.*, **2011**, *50*, 12232-12235. https://doi.org/10.1002/anie.201106046
30. Rapp, M.; Margas-Musielak, K.; Koroniak, H. *J. Fluorine Chem.*, **2015**, *179*, 142-149. https://doi.org/10.1016/j.jfluchem.2015.07.009
31. Shi, L.; Liu, Y.; Liu, Q.; Wei, B.; Zhang, G. *Green Chem.*, **2012**, *14*, 1372-1375. https://doi.org/10.1039/C2GC00006G
32. Kündig, E. P.; Enriquez-Garcia, A. *Beilstein J. Org. Chem.*, **2008**, *4*, 37. https://doi.org/10.3762/bjoc.4.37
33. Stankevič, M.; Pietrusiewicz, K. M. *Synlett*, **2003**, 1012-1016. https://doi.org/10.1055/s-2003-39304
34. Stankevič, M.; Jaklińska, M.; Pietrusiewicz, K. M. *J. Org. Chem.*, **2012**, *77*, 1991-2000. https://doi.org/10.1021/jo300026f
35. Stankevič, M.; Wójcik, K.; Jaklińska, M.; Pietrusiewicz, K. M. *Eur. J. Org. Chem.*, **2012**, 2521-2534. https://doi.org/10.1002/ejoc.201200096
36. Woźnicki, P.; Korzeniowska, E.; Stankevič, M. *J. Org. Chem.*, **2017**, *82*, 10271-10296. https://doi.org/10.1021/acs.joc.7b01767
37. Schirmer, M.-L.; Jopp, S.; Holz, J.; Spannenberg, A.; Werner, T. *Adv. Synth. Catal.*, **2016**, *358*, 26-29. https://doi.org/10.1002/adsc.201500762
38. Sowa, S.; Stankevič, M.; Flis, A.; Pietrusiewicz, K. M. *Synthesis*, **2018**, *50*, 2106-2118. https://doi.org/10.1055/s-0036-1591546
39. Kyne, S. H.; Lévêque, C.; Zheng, S.; Fensterbank, L.; Jutand, A.; Ollivier, C. *Tetrahedron*, **2016**, *72*, 7727-7737. https://doi.org/10.1016/j.tet.2016.08.039
40. R. G. Parr and W. Yang, Density-functional Theory of Atoms and Molecules. Oxford University Press, New York (1989).
41. Becke, A. D. *J. Chem. Phys.*, **1993**, *98*, 5648-5652. https://doi.org/10.1063/1.464913
42. Krishnan, R.; Binkley, J. S.; Seeger, R.; Pople, J. A. *J. Chem. Phys.*, **1980**, 72, 650-654. https://doi.org/10.1063/1.438955
43. Frisch, M. J.; Pople, J. A.; Binkley, J. S. *J. Chem. Phys.*, **1984**, *80*, 3265-3269. https://doi.org/10.1063/1.447079
44. Baker, J.; Woliński, K.; Malagoli, M.; Kinghorn, D.; Woliński, P.; Magyarfalvi, G.; Saebo, S.; Janowski, T.; Pulay, P. *J. Comput. Chem.*, **2009**, *30*, 317-335. https://doi.org/10.1002/jcc.21052